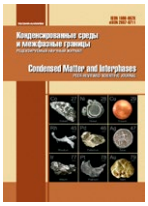

ISSN 1606-867X (Print)
ISSN 2687-0711 (Online)
Condensed Matter and Interphases
Kondensirovannye Sredy i Mezhfaznye Granitsy
https://journals.vsu.ru/kcmf/

Original articles

Research article
https://doi.org/10.17308/kcmf.2023.25/11168

Phase equilibra in the Ag_2S–Ag_8GeS_6–Ag_8SiS_6 system and some properties of solid solutions

G. M. Ashirov [1], K. N. Babanly[1], L. F. Mashadiyeva[1], Y. A. Yusibov[2], M. B. Babanly[1]✉

[1]*Institute of Catalysis and Inorganic Chemistry n.a. M. Nagiyev*
113 H. Javid av., Baku Az1143, Azerbaijan

[2]*Ganja State University ,*
Heydar Aliyev, 187, Ganja AZ2000, Ganja, Azerbaijan

Abstract

Phase equilibria in the Ag_2S–Ag_8SiS_6–Ag_8GeS_6 system were studied using differential thermal analysis and powder X-ray diffraction technique. Boundary section Ag_8SiS_6 – Ag_8GeS_6, liquidus surface projection, an isothermal section of the phase diagram at 300 K, and some polythermal sections of the studied system were constructed.

The formation of continuous series of solid solutions between both crystalline modifications of the starting compounds was determined in the Ag_8SiS_6–Ag_8GeS_6 system. The liquidus surface of the Ag_2S–Ag_8SiS_6–Ag_8GeS_6 system consists of two fields corresponding to the primary crystallization of the high-temperature modifications of the HT-$Ag_8Si_{1-x}Ge_xS_6$ and HT-Ag_2S phases. Lattice parameters for both modification of solid solutions were calculated based on powder X-ray diffraction data. The concentration dependence of lattice parameters obeys Vegard's rule.

The obtained new phases are of interest as environmentally safe materials with thermoelectric properties and mixed ion-electron conductivity.

Keywords: Argyrodite family compounds, Silver-germanium sulfide, Silver-silicon sulfide, Phase equilibria, Solid solutions, *T-x* diagram, Crystal structure

Acknowledgment: The work was financially supported by the Azerbaijan Science Foundation – Grant No AEF-MCG-2022-1(42)-12/10/4-M-10.

For citation: Ashirov G. M., Babanly K. N., Mashadiyeva L. F., Yusibov Y. A., Babanly M. B. Phase equilibra in the Ag_2S–Ag_8GeS_6–Ag_8SiS_6 system and some properties of solid solutions. *Condensed Matter and Interphases*. 2023;25(2): 292–301. https://doi.org/10.17308/kcmf.2023.25/11168

Для цитирования: Аширов Г. М., Бабанлы К. Н., Машадиева Л. Ф., Юсибов Ю. А., Бабанлы М. Б. Фазовые равновесия в системе Ag2S–Ag8GeS6–Ag8SiS6 и некоторые свойства твердых растворов. *Конденсированные среды и межфазные границы*. 2023;25(2): 292–301. https://doi.org/10.17308/kcmf.2023.25/11168

✉ Mahammad Babanly; email: babanlymb@gmail.com

1. Introduction

Binary and more complex chalcogenides of copper and silver are valuable functional materials [1-3]. Among these compounds, synthetic analogs of the argyrodite mineral with formula $A_8B^{IV}X_6$ (A – Cu, Ag; B^{IV} – Si, Ge, Sn; X – S, Se, Te) have high thermoelectric performance at low temperatures and are of special interest because they are environmentally safe [4–12]. At the same time, these compounds have semiconductor, photovoltaic, and optical properties [13–18]. On the other hand, the presence of highly concentrated and highly mobile Ag^+/Cu^+ ions distributed in a rigid anionic framework is ensured in the crystal structure of this class of compounds. Due to this feature of the crystal structure, some of the argyrodite compounds have high ionic conductivity for $Cu^+(Ag^+)$ cations, which makes them very promising for use in the preparation of photoelectrode materials, electrochemical solar energy converters, ion-selective sensors, etc. [19–22].

Study of new multicomponent materials is based on information about the phase equilibrium of the corresponding systems and the thermodynamic properties of the phases formed in them [23–26]. As the argyrodite family compounds are isostructural, there is a high probability of the formation of solid solutions in systems composed of these compounds. In [27–34], phase equilibria were studied in several systems consisting of argyrodite phases, and continuous series of solid solutions were found.

The present study aimed to obtain a complete picture of the phase equilibrium of the $Ag_2S–Ag_8GeS_6–Ag_8SiS_6$ composition area of the $Ag_2S–GeS_2–SiS_2$ quaternary system.

The primary compounds of the $Ag_2S–Ag_8GeS_6–Ag_8SiS_6$ system have been sufficiently studied. Ag_2S compound melts congruently at 1113 K and undergoes polymorphic transitions at 449 and 844 K [35]. Ag_8SiS_6 compound melts congruently at 1231 K and has a polymorphic transformation at 526 K [36]. Ag_8GeS_6 compound melts congruently at 1221 K [36] or 1223 K [37]. The polymorphic transition temperature of this compound is 488 K [36] or 496 K [37]. Both Ag_8SiS_6 and Ag_8GeS_6 low-temperature modifications crystallize in orthorhombic system (phase group $Pna2_1$) and the lattice parameters are as follows: Ag_8SiS_6: a = 15.024, b = 7.428, c = 10.533 Å[38]; Ag_8GeS_6: a = 15.149, b = 7.476, c = 10.589 Å [39].

High-temperature modifications of the ternary compounds have a cubic structure (phase group *F-43m*) with parameters: Ag_8SiS_6: a = 10.63 Å [38]; Ag_8GeS_6: a = 10.7 Å [40].

Ag_2S-Ag_8GeS_6 and Ag_2S-Ag_8SiS_6 quasi-binary boundary sections were reported in [35, 46]. Both systems form a eutectic-type diagram. Eutectic mixtures crystallize at 1080 K (20 mol%-Ag_8GeS_6) [35] and 1085 K (24 mol %-Ag_8SiS_6) [36].

The Ag_8GeS_6-Ag_8SiS_6 system has not been studied.

2. Experimental

2.1. Synthesis

Ag_2S, Ag_8SiS_6, and Ag_8GeS_6 compounds were synthesized by melting stoichiometric mixtures of the corresponding elements with high purity (no less 99.9999 %) in quartz ampoules under vacuum conditions (10^{-2}Pa). As the saturated vapor pressure of sulfur ($T_{boiling}$=717 K) is high at the melting temperature of all three compounds, their synthesis was carried out in a two-zone furnace. The furnace was gradually heated to a temperature of 40-50 K above the melting point of the synthesized compound. The part of the ampoule outside the oven is constantly cooled. Due to the process of cooling with water for 2–3 hours, the sulfur accumulated in the form of vapor at the end of the ampoule was condensed and sent to the reaction zone, and after absorbing most of the sulfur, the ampoule was completely inserted into the furnace. After keeping the ampoule in the furnace for 4–5 hours, they were gradually in the off-furnace mode.

The synthesized compounds were identified by differential thermal analysis (DTA) and X-ray diffraction (XRD) technique. Thus, the DTA results of Ag_2S, Ag_8SiS_6, and Ag_8GeS_6 compounds showed that their polymorphic transition and melting temperatures agree well with the literature data given above. X-ray diffraction analysis confirmed the homogeneity of the synthesized samples and the diffraction patterns of all three compounds agree with the literature data [19–28]. DTA and XRD results of the synthesized compounds are listed in the Table 1.

Alloys of the $Ag_2S–Ag_8GeS_6–Ag_8SiS_6$ system were prepared by melting mixtures of the

obtained starting compounds in different proportions in vacuumed quartz ampoules. To bring the samples to the equilibrium state, they were thermally treated for a long time (500 h) at 900 K. Two samples were prepared for each composition in the Ag_8GeS_6–Ag_8SiS_6 system, one of which was gradually cooled in a switched-off furnace after thermal treatment, and the other one was quenched by dropping the ampoule in cold water at 900 K.

2.2. Research methods

All the alloys were analyzed using powder XRD and DTA techniques. Powder XRD analysis was performed in a Bruker D2 PHASER diffractometer using CuKα1 radiation within the scanning range of 2θ = 5÷75. DTA measurements were recorded with a "Netzsch 404 F1 Pegasus system" differential scanning calorimeter (under flowing argon atmosphere) and a multichannel device based on the electronic "TC-08 thermocouple data logger" (in sealed quartz tubes). The measurement results were processed using the NETZSCH Proteus Software. The temperature measurement accuracy was within ±2 K.

3. Results and discussion

From the present experimental data and published reports on the Ag_2S–Ag_8GeS_6 and Ag_2S–Ag_8SiS_6 constituent binaries, we obtained a detailed picture of phase equilibria in the Ag_2S–Ag_8GeS_6–Ag_8SiS_6 system.

3.1. The border section Ag_8SiS_6-Ag_8GeS_6

Based on the DTA and XRD results, the phase diagram of the Ag_8SiS_6-Ag_8GeS_6 system was constructed. As can be seen from Fig. 1, continuous series of solid solutions are formed between both low (γ-phase) and high-temperature modifications (δ-phase) of the initial compounds. A special point of interest is that even though the melting temperatures (1231 and 1218 K) and polymorphic transformation temperatures (512 and 491 K) of the primary compounds are very close to each other, the extreme points on both the liquidus and solidus and δ ↔ γ phase transition curves not observed.

The lattice parameters of both ternary compounds and solid solutions were calculated using the TOPAS3.0 computer program and the results are listed in Table 1.

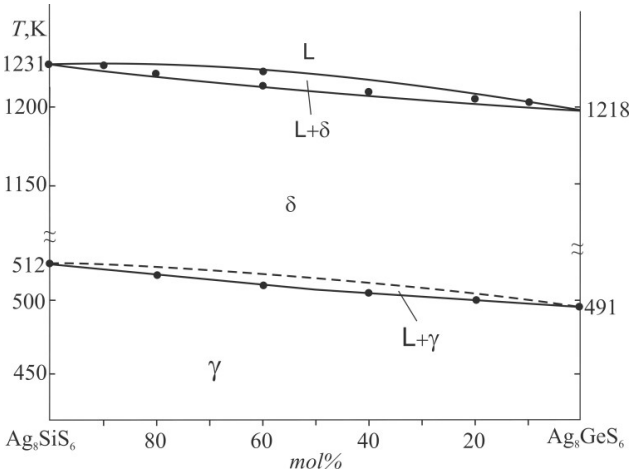

Fig. 1. Phase diagram of the Ag_8SiS_6-Ag_8GeS_6 system

Table 1. DTA and XRD results for Ag_8SiS_6 – Ag_8GeS_6 system

Composition, Mol % Ag_8GeS_6	Effect temperatures according to DTA data, K	Lattice parameters, Å ; low-temperature phase obtained by slow cooling to 298 K, (Sp. gr. *Pna2₁*)			Lattice parameters, Å; high temperature phase obtained by quenching from 900 K (Sp. gr. *F-43m*)
		a	*b*	*c*	*a*
0 (Ag_8SiS_6)	512 ; 1231	15.0264	7.4384	10.5311	10.6225
10	510 ; 1229	15.0524	7.4439	10.5411	10.6348
20	506 ; 1227	15.0751	7.4412	10.5429	10.6436
40	503 ; 1225-1228	15.0926	7.4523	10.5562	10.6552
60	499 ; 1223	15.0962	7.4601	10.5626	10.6785
80	497 ; 1121	15.1265	7.4694	10.5774	10.6935
90	494 ; 1219	15.1345	7.4705	10.5823	10.7026
100	491 ; 1218	15.1442	7.4713	10.5912	10.7124

Ag_8GeS_6 and Ag_8SiS_6 compounds both have orthorhombic structure under room conditions (space group- Pna_{21}). The high-temperature modifications of both compounds are cubic (phase group F-43m). Table 1 lists the thermal effects and crystal lattice parameters of the starting compounds and solid solutions.

Graphs of the dependence of crystal lattice parameters on concentration were constructed (Fig. 2). As can be seen, the lattice parameters of both modifications of solid solutions increase linearly with Ge substitution, i.e., they follow Vegard's rule.

Fig. 3 shows powder diffraction patterns of thermally treated and slowly cooled alloys. As can be seen, all intermediate alloys have the same diffraction pattern as the starting compounds. This indicates the formation of continuous series of solid solutions in the Ag_8SiS_6–Ag_8GeS_6 system between room temperature modifications of the starting compounds over the entire consentration range. A slight shift of the diffraction lines towards small angles is observed because of Si → Ge substitution. This is because the ionic radius of germanium is larger than silicon.

Fig. 4 shows powder XRD patterns of Ag_8SiS_6 – Ag_8GeS_6 alloys quenched at 900 K. Analysis of the XRD patterns of the quenched alloys shows the formation of continuous series of solid solutions between high-temperature modifications in the entire range. As can be seen, the diffraction patterns of high-temperature alloys have a

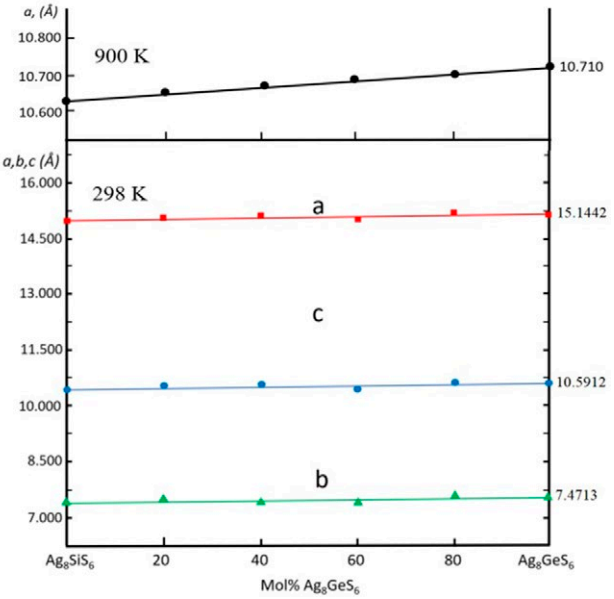

Fig. 2. Dependences of lattice parameters of the low-temperature (stable at room temperature) and high-temperature modifications of Ag_8SiS_6 – Ag_8GeS_6 solid solutions on composition

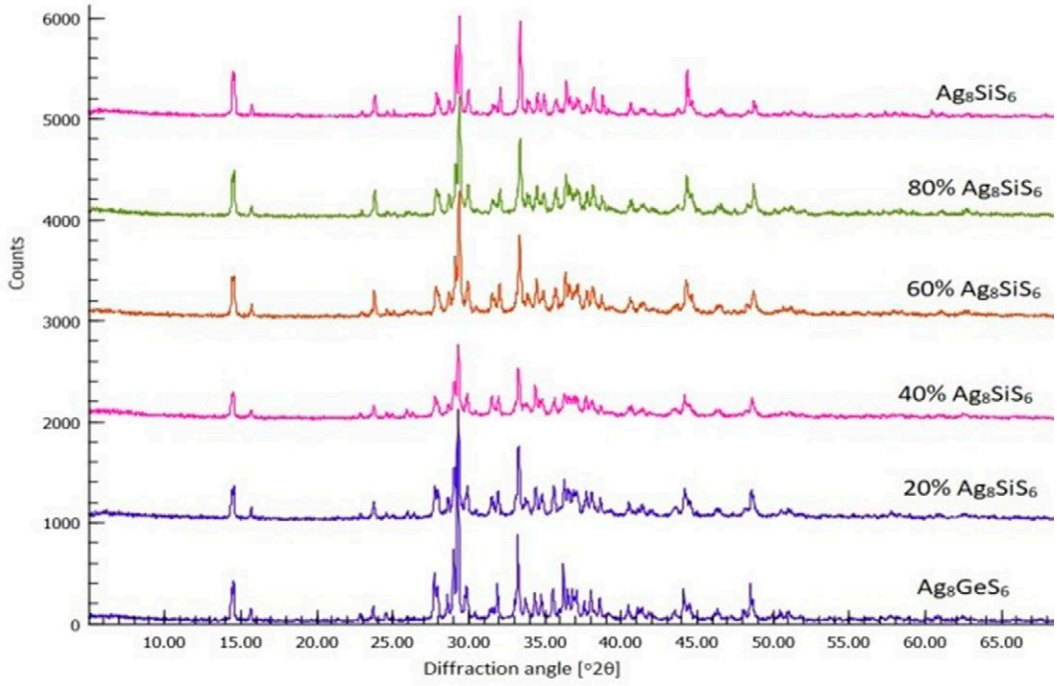

Fig. 3. Powder XRD patterns of the Ag_8SiS_6 – Ag_8GeS_6 alloys (slowly cooled to room temperature samples)

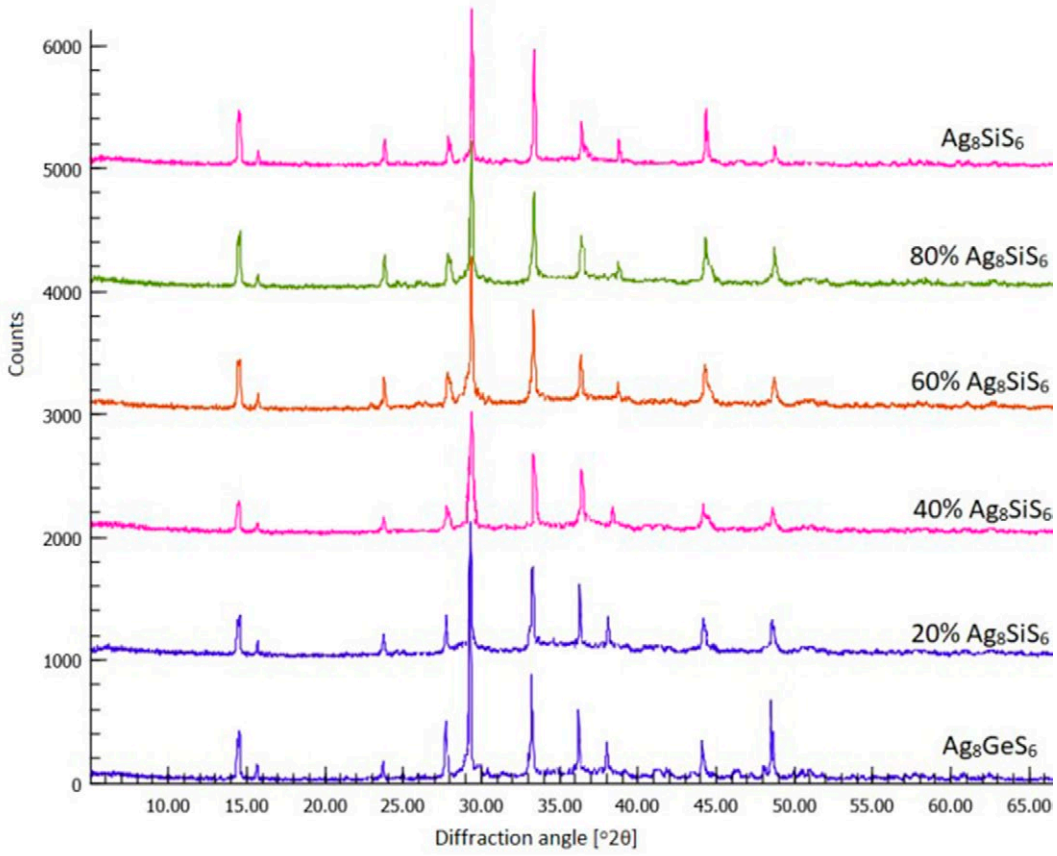

Fig. 4. Powder XRD patterns of Ag_8SiS_6 – Ag_8GeS_6 alloys (quenched at 900 K samples)

diffraction pattern characteristic of a cubic structure.

3.2. Solid phase equilibria in the $Ag_2S–Ag_8GeS_6–Ag_8SiS_6$ system at 300 K

Based on the XRD results of a number of equilibrium alloys within the $Ag_2S–Ag_8GeS_6–Ag_8SiS_6$ concentration triangle and the phase diagrams of boundary quasi-binary systems, a solid phase equilibria diagram of this system at 300 K was constructed (Fig. 5). The formation of the γ-phase in the $Ag_8GeS_6–Ag_8SiS_6$ boundary system, and the absence of other phases in the concentration triangle lead to the formation of a two-phase α′+γ field (where α′ is a solid solution formed on the basis of low-temperature Ag_2S). Connode lines are formed between α′ and γ-phases. The phase composition of room temperature alloys of the $Ag_2S–Ag_8GeS_6–Ag_8SiS_6$ system was determined by XRD. Fig. 5 shows the studied vertical sections and the composition of the alloys. For example, the diffraction patterns and phase compositions of alloys 1 and 2 from Fig. 5 are shown in Fig. 6. As can be seen, the diffraction patterns of both alloys consist of the sum of the diffraction lines of the low-temperature modification of Ag_2S and the γ-phase.

3.3. Liquidus surface projection of the $Ag_2S–Ag_8GeS_6–Ag_8SiS_6$ system

The liquidus surface projection of this system consists of two fields, which correspond to the primary correspond to the primary crystallization of the δ-phase and α solid solutions based on the high-temperature modification of the Ag_2S compound (Fig. 7). These fields are bounded by the e1e2 monovariant eutectic curve:

$$L \leftrightarrow \alpha + \delta. \qquad (1)$$

3.4. Some polythermal sections of the phase diagram

The Ag_2S-[A] section ([A] – $Ag_8Si_{0.5}Ge_{0.5}Se_6$ solid solution). The liquidus of this section (Figure 8) consists of two curves of primary crystallization fields of α and δ solid solutions.

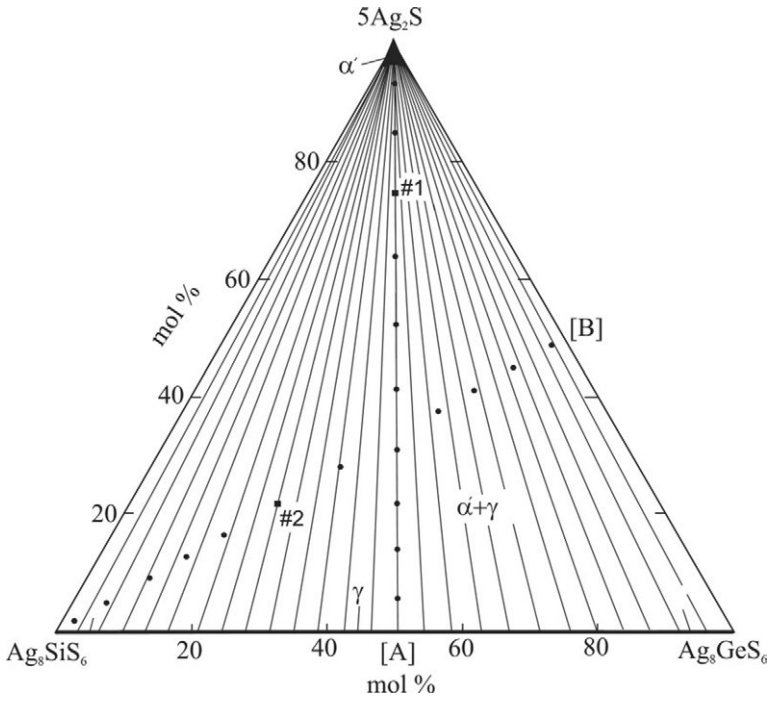

Fig. 5. Isothermal section of the Ag_2S–Ag_8SiS_6–Ag_8GeS_6 system at 300 K

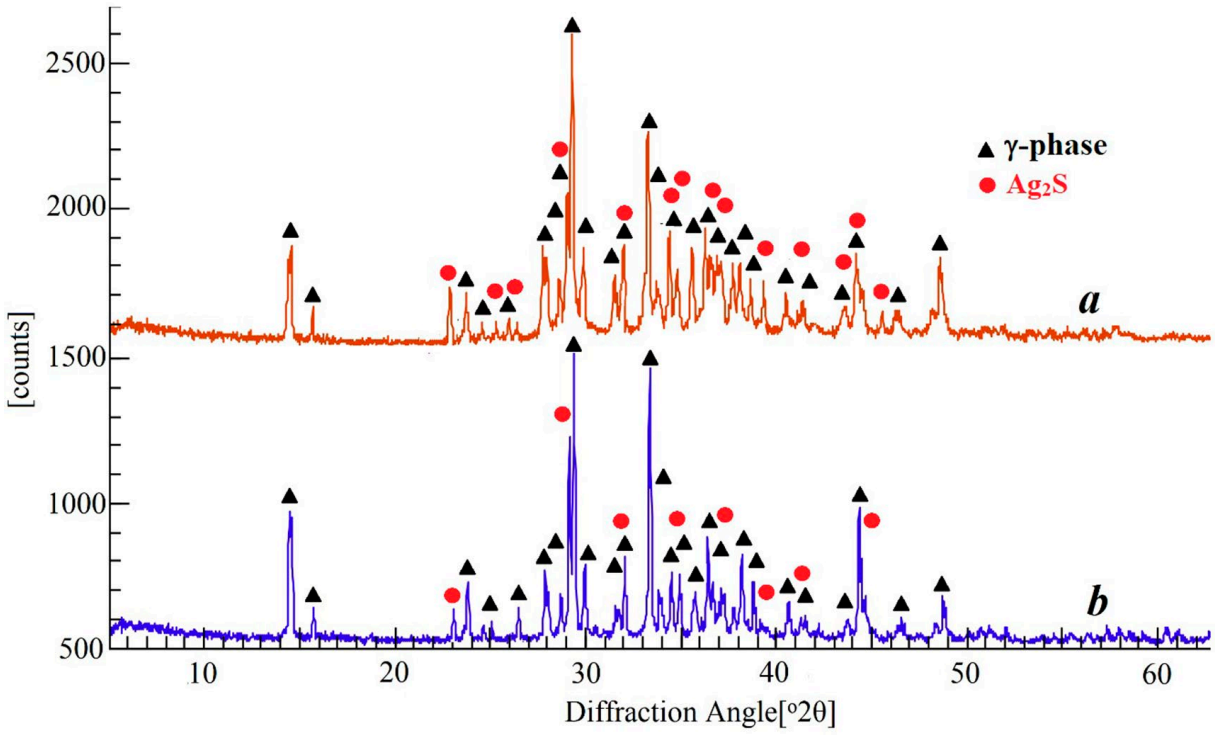

Fig. 6. Powder XRD patterns (300 K) of Ag_2S–Ag_8SiS_6–Ag_8GeS_6 alloys: (a) alloy – #1 and (b) alloy – #2 in Fig. 5

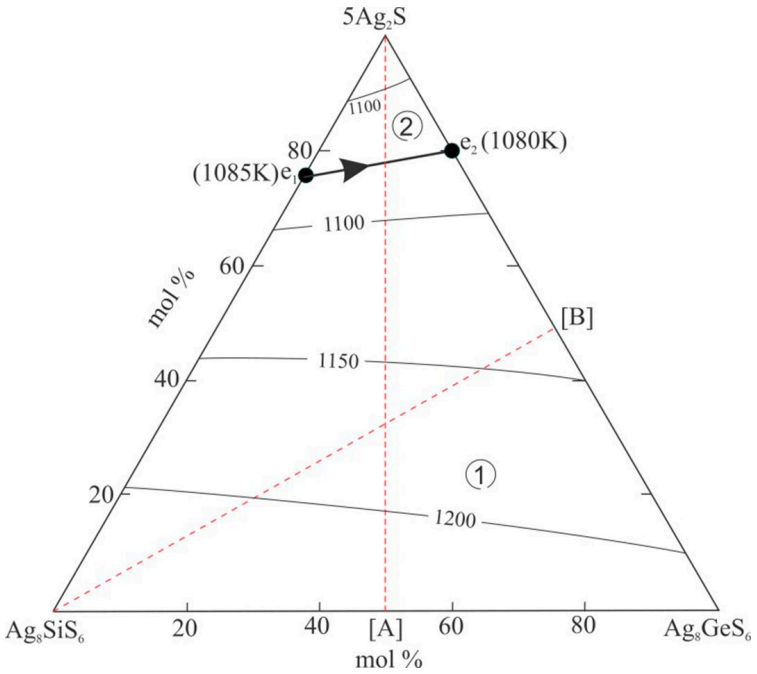

Fig. 7. The liquidus surface projection of the Ag_2S–Ag_8GeS_6–Ag_8SiS_6 system. Primary crystallization fields: *1* (δ), *2* (α). Dashed lines indicate studied sections

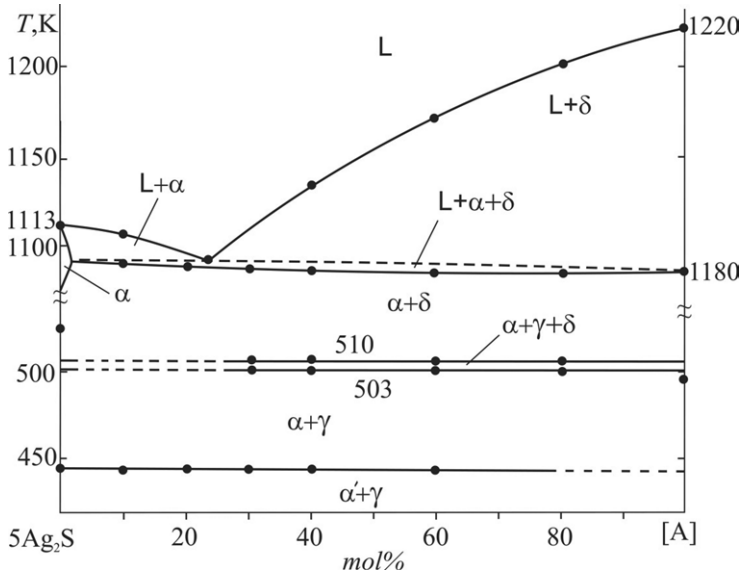

Fig. 8. Polythermal section Ag_2S–[A] ([A] – $Ag_8Si_{0.5}Ge_{0.5}Se_6$ solid solution)

The crystallization process ends with the formation of the two-phase field α + δ. Below the liquidus, crystallization proceeds according to the eutectic reaction (1). Since the temperatures of e1 and e2 eutectic equilibria on Ag_2S–Ag_8SiS_6 and Ag_2S– Ag_8GeS_6 boundary systems differ little (Fig. 7), the temperature interval of this monovariant eutectic equilibrium is very small (2–3°). Therefore, in Figure 8, the L + α + δ three-phase field is delimited by a dotted line. Thermal effects at the 503–510 K range correspond to monovariant equilibrium δ ↔ α + γ. There is no more than 5% solubility area based on the high-temperature modification of Ag_2S. The horizontal line at 443K corresponds to the polymorph transformation α ↔ α′.

The Ag_8SiS_6–[B] Ag_2S–[A] section ([B] is alloy of the $5Ag_2S$–Ag_8GeS_6 system containing 50 mol % Ag_8GeS_6). This section is entirely located in the primary crystallization field of the δ-phase (Fig. 9)

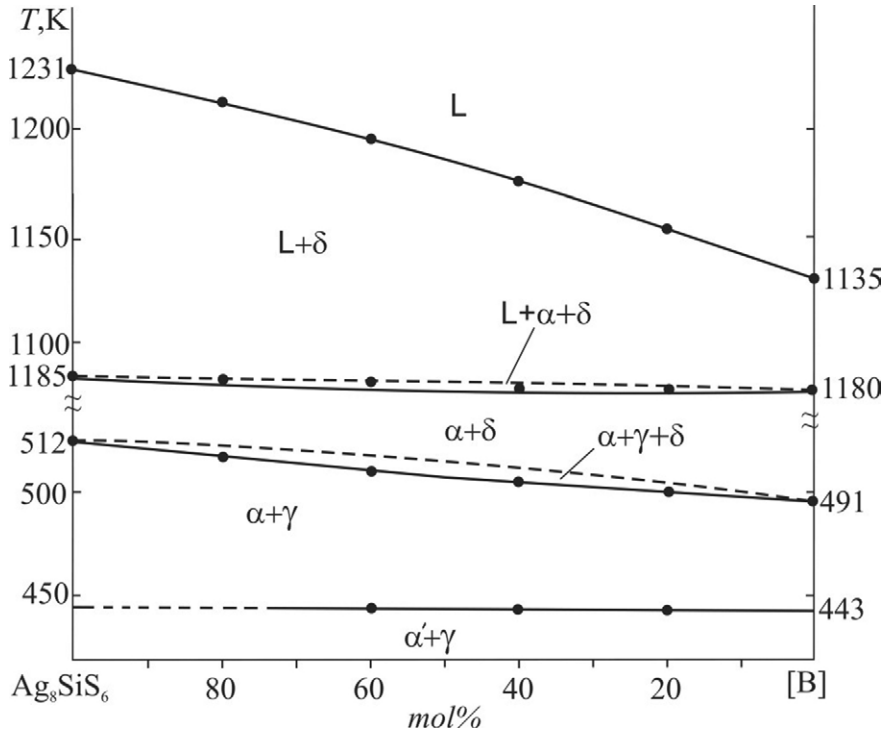

Fig. 9. Polythermal section Ag_8SiS_6–[B] section. ([B] – is alloy of the $5Ag_2S$–Ag_8GeS_6 system containing 50%mol Ag_8GeS_6)

and firstly δ-solid solutions crystallize from the liquid phase. Crystallization continues according to the monovariant eutectic reaction (1) and ends with the formation of two-phase mixtures α + δ. Then δ ↔ α + γ monovariant eutectoid reaction (512–491) and polymorphic transformation of Ag_2S (443 K) take place.

3. Conclusion

The phase equilibria of the Ag_2S–Ag_8SiS_6–Ag_8GeS_6 plane of the Ag–Si–Ge–S system were studied. The liquidus surface projection of the mentioned subsystem, solid phase equilibria diagram at 300 K, as well as two polythermal sections of the phase diagram were constructed. It was determined that continuous series of solid solutions are formed between both crystallographic modifications of the starting compounds in the boundary Ag_8SiS_6–Ag_8GeS_6 system. Based on powder diffractograms, the homogeneity of both solid solutions was confirmed, and their crystal lattice types and parameters were determined. It is shown that the dependence of the lattice parameters on the composition obeys Vegard's rule. The obtained new non-stoichiometric phases are of particular interest as environmentally safe, thermoelectric, and mixed ion-electron conducting materials.

Author contributions

G. M. Ashirov – research concept, conducting research, synthesis of compounds, article writing, discussion of results. L. F. Mashadiyeva – analysis of scientific literature, discussion of results. K. N. Babanly – discussion of results. Y. A. Yusibov – discussion of results. M. B. Babanly – research concept, final conclusions.

Conflict of interests

The authors declare that they have no known competing financial interests or personal relationships that could have influenced the work reported in this paper.

Referenses

1. Sanghoon X. L., Tengfei L. J., Zhang L. Y. *Chalcogenides: From 3D to 2D and beyond*. Elsevier; 2019. 398 p.

2. Ahluwalia G. K. *Applications of chalcogenides: S, Se, and Te*. Springer; 2016. 461 p.

3. Fujikane M., Kurosaki K., Muta H., Yamanaka S.. Thermoelectric properties of α- and β-Ag_2Te. *Journal of Alloys and Compounds*. 2005;393(1-2): 299–301. https://doi.org/10.1016/j.jallcom.2004.10.002

4. Schwarzmüller S., Souchay D., Günther D., … Oeckler O. Argyrodite-type Cu_8GeSe_6-x Te x($0 \leqslant x \leqslant 2$): temperature-dependent crystal structure and thermoelectric properties. *Zeitschrift für anorganische und allgemeine Chemie*. 2018;644(24): 1915–1922. https://doi.org/10.1002/zaac.201800453

5. Acharya S., Soni A. High thermoelectric power factor in *p*-type Cu_8GeSe_6. *DAE Solid State Physics Symposium 2018*. 2019;2115(1): 1–3. https://doi.org/10.1063/1.5113463

6. Li W., Lin S., Ge B., Yang J., Zhang W., Pei Y. Low sound velocity contributing to the high thermoelectric performance of Ag_8SnSe_6. *Advanced Science*. 2016;3(11): 1600196. https://doi.org/10.1002/advs.201600196

7. Ghrib T., Al-Otaibi A. L., Almessiere M. A., Assaker I. B., Chtourou R. High thermoelectric figure of merit of Ag_8SnS_6 component prepared by electrodeposition technique. *Chinese Physics Letters*. 2015;32(12: 127402. https://doi.org/10.1088/0256-307x/32/12/127402

8. Jin M., Lin S., Li W., … Pei Y. Fabrication and thermoelectric properties of single-crystal argyrodite Ag_8SnSe_6. *Chemistry of Materials*. 2019;31(7): 2603–2610. https://doi.org/10.1021/acs.chemmater.9b00393

9. Shen X., Yang C.-C., Liu Y., Wang G., Tan H., Tung Y.-H., Zhou X.. High-temperature structural and thermoelectric study of argyrodite Ag_8GeSe_6. *ACS Applied Materials & Interfaces*. 2018;11(2): 2168–2176. https://doi.org/10.1021/acsami.8b19819

10. Charoenphakdee A., Kurosaki K., Muta H., Uno M., Yamanaka S. Ag_8SiTe_6: A new thermoelectric material with low thermal conductivity. *Japanese Journal of Applied Physics*. 2009;48(1): 01160–01169. https://doi.org/10.1143/jjap.48.011603

11. Jiang Q., Li S., Luo Y., Xin J., Li S., Li W., Yang J. Ecofriendly highly robust Ag_8SiSe_6-based thermoelectric composites with excellent performance near room temperature. *ACS Applied Materials & Interfaces*. 2020;12(49): 54653–54661. https://doi.org/10.1021/acsami.0c15877

12. Fujikane M., Kurosaki K., Muta H., Yamanaka S. Thermoelectric properties of Ag_8GeTe_6. *Journal of Alloys and Compounds*. 2005;396(1-2): 280–282. https://doi.org/10.1016/j.jallcom.2004.12.038

13. Semkiv I., Ilchuk H., Pawlowski M., Kusnezh V. Ag_8SnSe_6 argyrodite synthesis and optical properties. *Opto-Electronics Review*. 2017;25(1): 37–40. https://doi.org/10.1016/j.opelre.2017.04.002

14. Lu C.-L., Zhang L., Zhang Y.-W., Liu S.-Y., Mei Y. Electronic, optical properties, surface energies and work functions of Ag_8SnS_6: First-principles method. *Chinese Physics B*. 2015;24(1): 017501. https://doi.org/10.1088/1674-1056/24/1/017501

15. Boon-on P., Aragaw B. A., Lee C.-Y., Shi J.-B., Lee M.-W. Ag_8SnS_6: a new IR solar absorber material with a near optimal bandgap. *RSC Advances*. 2018;8(69): 39470–39476. https://doi.org/10.1039/c8ra08734b

16. Brammertz G., Vermang B., ElAnzeery H., Sahayaraj S., Ranjbar, S., Meuris M., Poortmans J. Fabrication and characterization of ternary Cu_8SiS_6 and Cu_8SiSe_6 thin film layers for optoelectronic applications. *Thin Solid Films*. 2016;616: 649–654. https://doi.org/10.1016/j.tsf.2016.09.049

17. Acharya S., Pandey J., Soni A. Enhancement of power factor for inherently poor thermal conductor Ag_8GeSe_6 by replacing Ge with Sn. *ACS Applied Energy Materials*. 2019;2(1): 654–660. https://doi.org/10.1021/acsaem.8b01660

18. Tim B., Riley H., Bjoern W., … Wolfgang G. Z. Considering the role of ion transport in diffuson-dominated thermal conductivity. *Advanced Energy Materials*. 2022;12: 2200717. https://doi.org/10.1002/aenm.202200717

19. Hull S., Berastegui P., Grippa A. Ag^+ diffusion within the rock-salt structured superionic conductor $Ag_4Sn_3S_8$. *Journal of Physics: Condensed Matter*. 2005;17(7): 1067–1084. https://doi.org/10.1088/0953-8984/17/7/002

20. Heep B. K., Weldert K. S., Krysiak Y., … Tremel W. High electron mobility and disorder induced by silver ion migration lead to good thermoelectric performance in the argyrodite Ag_8SiSe_6. *Chemistry of Materials*. 2017;29(11): 4833–4839. https://doi.org/10.1021/acs.chemmater.7b00767

21. Boucher F., Evain M., Brec R. Distribution and ionic diffusion path of silver in γ-Ag_8GeTe_6: A temperature dependent anharmonic single crystal structure study. *Journal of Solid State Chemistry*. 1993;107(2): 332–346. https://doi.org/10.1006/jssc.1993.1356

22. Sardarly R. M., Ashirov G. M., Mashadiyeva L. F., … Babanly M. B. Ionic conductivity of the Ag_8GeSe_6 compound. *Modern Physics Letters B*. 2023;36(32): 2250171. https://doi.org/10.1142/S0217984922501718

23. West D. R. F. *Ternary phase diagrams in materials science*. 3rd edition. CRC Press; 2019. 236 p.

24. Saka Hiroyasu. *Introduction to phase diagrams in materials science and engineering*. World Scientific Publishing Company; 2020. 188 p. https://doi.org/10.1142/11368

25. Babanly M. B., Mashadiyeva L. F., Babanly D. M., Imamaliyeva S. Z., Taghiyev D. B., Yusibov Y. A. Some issues of complex investigation of the phase equilibria and thermodynamic properties of the ternary chalcogenide systems by the EMF method. *Russian Journal of Inorganic Chemistry*. 2019;64(13): 1649–1671. https://doi.org/10.1134/s0036023619130035

26. Imamaliyeva S. Z., Babanly D. M., Tagiev D. B., Babanly M. B. Physicochemical aspects of development of multicomponent chalcogenide phases having the

Tl_5Te_3 structure: A Review. *Russian Journal of Inorganic Chemistry*. 2018;63(13): 1703–1730. https://doi.org/10.1134/s0036023618130041

27. Mashadieva L. F., Alieva Z. M., Mirzoeva R. D. Yusibov Yu. A. A., Shevel'kov V. , Babanly M. B. Phase equilibria in the $Cu_2Se–GeSe_2–SnSe_2$ system. *Journal of Inorganic Chemistry*. 2022;67: 670–682. https://doi.org/10.1134/S0036023622050126

28. Alverdiyev I. J., Aliev Z. S., Bagheri S. M., Mashadiyeva L. F., Yusibov Y. A., Babanly M. B. Study of the $2Cu_2S+GeSe_2 \leftrightarrow Cu_2Se+GeS_2$ reciprocal system and thermodynamic properties of the $Cu8GeS_6$-xSex solid solutions. *Journal of Alloys and Compounds*. 2017;691: 255–262. https://doi.org/10.1016/j.jallcom.2016.08.251

29. Alverdiev I. J., Bagheri S. M., Aliyeva Z. M., Yusibov Y. A., Babanly M. B. Phase equilibria in the $Ag_2Se–GeSe_2–SnSe_2$ system and thermodynamic properties of $Ag_8Ge_{1-x}Sn_xSe_6$ solid solutions. *Inorganic Materials*. 2017;53(8), 786–796. https://doi.org/10.1134/s0020168517080027

30. Aliyeva Z. M., Bagheri S. M., Aliev Z. S., Alverdiyev I. J., Yusibov Y. A., Babanly M. B. The phase equilibria in the $Ag_2S–Ag_8GeS_6–Ag_8SnS_6$ system. *Journal of Alloys and Compounds*.2014;611: 395–400. https://doi.org/10.1016/j.jallcom.2014.05.112

31. Bagheri S. M., Imamaliyeva S. Z., Mashadiyeva L. F., Babanly M. B. Phase equilibria in the Ag_8SnS_6-Ag_8SnSe_6 system. *International Journal of Advanced Scientic and technical Research (India)*. 2014;4(2): 291–296.

32. Bayramova U. R., Poladova A. N., Mashadiyeva L. F. Synthesis and X-RAY study of the $Cu_8Ge_{(1-X)}Si_XS_6$ solid solutions. *New Materials, Compounds & Applications*. 2022;6(3): 276–281.

33. Alieva Z. M., Bagkheri S. M., Alverdiev I. J., Yusibov Y. A., Babanly M. B. Phase equilibria in the pseudoternary system $Ag_2Se–Ag_8GeSe_6–Ag_8SnSe_6$. *Inorganic Materials*. 2014;50(10): 981–986. https://doi.org/10.1134/s002016851410001x

34. Ashirov G. M. Phase equilibria in the $Ag_8SiTe_6–Ag_8GeTe_6$ system. *Azerbaijan Chemical Journal*. 2022;1: 89–93. https://doi.org/10.32737/0005-2531-2022-1-89-93

35. Olekseyuk I. D., Kogut Y. M., Fedorchuk A. O., Piskach L. V., Gorgut G. P., Parasyuk O. V. The $Ag_2S–GeS_2$ system and Ag_2GeS_3 crystal structure. *Naukovyi visnyk Volyns'koho Natsional'noho Universytetu im. Lesi Ukrainky. Neorhanichna Khimiia*. 2010;16: 25–33.

36. Venkatraman M., Blachnik R., Schlieper A. The phase diagrams of M_2X-SiX_2 (M is Cu, Ag; X is S, Se). *Thermochimica Acta*. 1995;249: 13–20. https://doi.org/10.1016/0040-6031(95)90666-5

37. Mikolaichuk A. G., Moroz N. V. *T-x* diagram of the Ag-Ge-S system in the Ag-Ge-GeS_2-Ag_8GeS_6-Ag region: The glassy crystalline state of alloys. *Russian Journal of Inorganic Chemistry*. 2010;55(1): 87–92. https://doi.org/10.1134/S0036023610010171

38. Krebs B., Mandt J. Zur Kenntnis des argyrodit-strukturtyps: die kristallstruktur von Ag_8SiS_6 / The argyrodite structure type : The crystal structure of Ag_8SiS_6. *Zeitschrift Für Naturforschung B*. 1977; 32(4): 373–379. https://doi.org/10.1515/znb-1977-0404

39. Eulenberger G. Die kristallstruktur der tieftemperaturmodifikation von Ag_8GeS_6 – synthetischer argyrodit. *Monatshefto für Chemie*. 1977;108: 901–913. https://doi.org/10.1007/BF00898056

40. Gorochov O. Les composés Ag_8MX_6 (M= Si, Ge, Sn et X= S, Se, Te). *Bull. Soc. Chim. France*. 1968;6: 2263–2275

Information about of authors

Garay M. Ashirov, PhD student, Researcher, *Institute of Catalysis and Inorganic Chemistry* named after academician *Murtuza* Naghiyev (Baku, Azerbaijan).

https://orcid.org/0000-0001-5050-9858

garayasirov@gmail.com

Kamala N.Babanly, PhD in Chemistry, Senior Researcher, *Institute of Catalysis and Inorganic Chemistry* named after academician *Murtuza* Naghiyev (Baku, Azerbaijan).

https://orcid.org/0000-0002-3275-5833

leylafm@rambler.ru

Leyla F. Mashadiyeva, PhD in Chemistry, Senior Researcher, *Institute of Catalysis and Inorganic Chemistry* named after academician *Murtuza* Naghiyev (Baku, Azerbaijan).

https://orcid.org/0000-0003-2357-6195

leylafm76@gmail.com

Yusif A. Yusibov, DSc in Chemistry, Professor, Rector of the Ganja State University

https://orcid.org/0000-0003-4081-6170

babanlymb@gmail.com

Mahammad B. Babanly, DSc in Chemistry, Professor, Associate Member of the Azerbaijan National Academy of Sciences, Executive Director of the *Institute of Catalysis and Inorganic Chemistry* named after academician *Murtuza* Naghiyev (Baku, Azerbaijan).

https://orcid.org/0000-0001-5962-3710

babanlymb@gmail.com

Received 05.10.2022; approved after reviewing 24.11.2022; accepted for publication 15.15.2022; published online 25.06.2023.

Translated by author